

Influence of Externally Applied Bias and Atomic Hydrogen Formation on the Properties of Nanocrystalline Silicon Deposited by Expanding Thermal Plasma Chemical Vapor Deposition

R. Jimenez Zambrano, R. A. C. M. M. van Swaaij, M. C. M van de Sanden, and M. Zeman

Abstract— Nanocrystalline silicon (nc-Si:H) deposited with ETP-CVD shows a high degree of porosity. In this paper the underlying reasons for this porosity are investigated, using infrared absorption measurements, optical emission spectroscopy, and spectroscopic ellipsometry. The influence of applying RF biasing on the substrate is investigated. In that case material with a higher density is obtained, which is ascribed to a higher surface mobility of radicals on the film surface during growth as a result of higher atomic hydrogen formation, ion bombardment and to modifications in the mechanism of cluster incorporation. The results suggest that this porosity is due to a lack of atomic hydrogen formed close to the growing surface. The position where the hydrogen feed gas is injected influences the porosity of the material, as in this way the atomic H concentration near the growing film surface is increased.

Index Terms—Semiconductor growth, Infrared spectroscopy, Hydrogen, Chemical vapor deposition.

I. INTRODUCTION

AMORPHOUS and nanocrystalline silicon (a-Si:H and nc-Si:H) are materials with demonstrated properties for photovoltaic application. These materials are expected to be used for mass production of cheap and high efficient solar cells. Due to the low absorption of nc-Si:H a thick layer ($> 1 \mu\text{m}$) is required, which renders the deposition rate a crucial parameter. Several techniques are used to grow nc-Si:H at high deposition rates. Promising results have been

achieved by very high frequency (VHF) plasma-enhanced chemical vapor deposition (PECVD) in the high-pressure depletion (HPD) regime [1,2] and VHF-PECVD in a triode-reactor configuration [1]. The combination of VHF-PECVD and HPD achieves high deposition rates due to an efficient dissociation of feed gases together with a decrease in ion energy and an increase in ion flux at higher frequencies. With this technique nc-Si:H solar cells with 9.9% efficiency at 0.45 nm/s and 6.4% at 4.5 nm/s have been obtained [2]. Using the triode reactor configuration nc-Si:H solar cells with 3.4% efficiency at 6 nm/s have been deposited [3].

Expanding thermal plasma chemical vapor deposition (ETP-CVD) is a remote plasma technique characterized by high deposition rates and low-energy ion bombardment. In this technique plasma is created in a cascaded arc at high pressure and this plasma then expands into the reactor that is maintained at lower pressure. It was reported earlier that with this technique nc-Si:H could be grown at 3.7 nm/s [4]. Also it was shown that the material properties of nc-Si:H could be influenced significantly by moving the injection ring towards the substrate [5], though the results suggested that the mix of depositing radicals did not change when moving the injection ring [6]. The initial implementation of nc-Si:H in solar cells shows that porous material with crack-like voids is deposited with ETP-CVD [7]. So far, the porosity of the nc-Si:H is a characteristic systematically observed when using ETP-CVD [11].

In this paper we will study the causes of the porosity and we will study the changes in porosity with bias and hydrogen injection position. First, ETP-CVD is described briefly and subsequently the different experimental results are presented and discussed. The paper will conclude with remarks.

II. EXPERIMENT

The films were deposited by ETP-CVD, a remote plasma technique in which plasma is created in the cascaded arc at high pressure (0.2 to 0.5 bar). In our vertical configuration, the arc is located above the substrate. Via a nozzle the plasma

Manuscript received September 29, 2007. (Write the date on which you submitted your paper for review.) This work was supported by SenterNovem.

R. Jimenez Zambrano is with the Delft University of Technology, DIMES-ECTM, P. O. Box 5053, 2600 GB Delft, The Netherlands (phone: +31152787307; fax: +31152622163; e-mail: r.jimenezzambrano@tudelft.nl)

R. A. C. M. M. van Swaaij is with the Delft University of Technology, DIMES-ECTM, P. O. Box 5053, 2600 GB Delft, The Netherlands (e-mail: r.a.c.m.m.vanswaaij@tudelft.nl)

M. C. M van de Sanden is with the University of Technology, Department of Applied Physics, P. O. Box 513, 5600 MB Eindhoven, The Netherlands (e-mail: M.C.M.v.d.Sanden@phys.tue.nl)

M. Zeman is with the Delft University of Technology, DIMES-ECTM, P. O. Box 5053, 2600 GB Delft, The Netherlands (e-mail: m.zeman@tudelft.nl)

expands to a reactor at lower pressure (~ 0.2 mbar), where the atomic hydrogen emanating from the arc reacts with SiH_4 injected further down into the expanding plasma through an injection ring. Due to the limited pumping capacity the reactor pressure is determined by the total gas flow. The depositions were performed at pressures between 0.12 and 0.28 mbar. The current through the cascaded arc plasma was 35 A. The hydrogen can be injected in the arc, the nozzle and/or the injection ring. The hydrogen flow injected into the arc was kept constant to maintain the same plasma conditions. In a first series of experiments the hydrogen flow injected in the nozzle was varied to control the dilution. In a second set of experiments, similar hydrogen flows were injected through the injection ring instead of the nozzle. The main difference between the nozzle and the injection ring is the position with respect to the substrate holder. The nozzle is located 45 cm while the injection ring is located 5.5 cm above the substrate holder. The substrate temperature was 200°C. Further, the substrate can be biased independently to control the ion bombardment by applying a 13.5-MHz RF signal to the substrate with the walls of the reactor as ground. The power varied between 0 and 30 W. When an RF voltage is applied to the substrate in combination with ETP-CVD, the substrate potential consists of two parts: a DC voltage, V_{dc} , and an AC voltage. With the frequency used, the DC voltage determines the energy of the impinging ions. Films of 500 nm were grown on Corning 1737 glass and on one-side-polished monocrystalline Si wafer with native oxide.

The temporal evolution of the material was followed in situ by Spectroscopy Ellipsometry (SE) and Optical Emission Spectroscopy (OES). SE measurements were carried out using a J. A. Woollam Co., Inc M-2000F rotating compensator spectroscopic ellipsometer. Control of the measurement setup and data acquisition were done via WVASE provided by J. A. Woollam Co., Inc. Spectra were collected from 250 to 1000 nm in 470 separate channels. The angle of incidence was about 68° and the light beam passed through non-strain free windows, so a window effect had to be included in the data analysis. For all in-situ experiments 8 measurements were averaged, resulting in a time resolution of about 1.8 seconds. The OES system consists of an AvaSpec-3648 spectrometer connected to the reactor chamber through a 20-cm long arm

flowed with He. A shutter and two slides are installed inside the arm to reduce deposition on the quartz crystal, which seals the arm. The OES system is aligned parallel to the substrate holder. Four emission lines were simultaneously monitored: Si^* [288 nm], SiH^* [414 nm], H_α [656 nm] and H_β [486 nm].

The IR-absorption measurements between 400 and 6000 cm^{-1} wave numbers were performed with a Nicolet 6700 FT-IR spectrometer on films deposited on crystalline Si wafers. The wave-number range from 2000-6000 cm^{-1} was used to determine the thickness of the sample accurately, which in turn was used to calculate the absorption coefficient and the hydrogen concentration. To analyze the FTIR spectra in the region 800-950 cm^{-1} we have followed the assignment of these peaks reported in Ref. [8]. For the region 1800-2200 cm^{-1} we have followed Ref. [9]. The modes analyzed are separated between bulk and surface modes, where the surface modes originate from dangling bonds terminated by hydrogen at the inner surfaces of voids. From the IR-absorption, we determine the microstructure factor, R^* , which is defined as the ratio of the areas of the multihydrides in the bulk to monohydrides and multihydrides in the bulk. To determine the crystalline fraction, f_c , of the films deposited on glass we used a Renishaw InVia Raman microscope with a 514-nm Ar laser. In order to obtain f_c , first three peaks are used to fit the amorphous part of the Raman spectrum (not including from 470 to 540 cm^{-1}). Afterwards, the amorphous part is subtracted from the measurement. The remaining spectrum is associated with the nanocrystalline part of the material and is fitted with two modes at 510 and 520 cm^{-1} . The crystalline fraction is then calculated as $f_c = (I_{510} + I_{520}) / (0.8 \cdot I_{480} + I_{510} + I_{520})$.

III. RESULTS AND DISCUSSION

A. External RF biasing

In a previous study [11] we have shown the influence of external RF biasing on the densification of the material. Figure 1 compares the IR absorption spectra of two dilution series, the first without RF biasing (Fig. 1(a)) and the second, similar to the first one, but now with RF biasing (Fig. 1(b)).

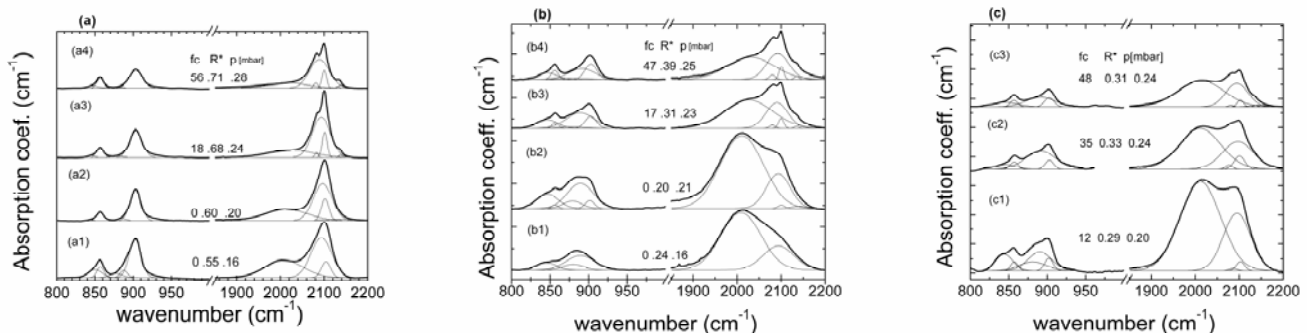


Fig. 1. FT-IR absorption spectra of nc-Si:H films prepared at several H_2 flow conditions: (a) without RF bias and H_2 injected through the nozzle, (b) with RF bias and H_2 injected through the nozzle, (c) with RF bias and H_2 injected through the injection ring. These flows result in different crystalline factors (f_c) and microstructure factors (R^*) at different deposition pressure (see text), given in the graphs.

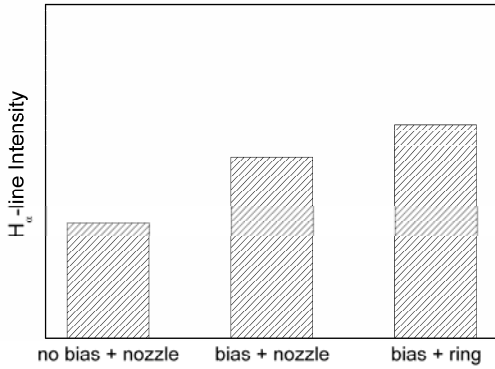


Fig. 2. OES emission intensity of H_{α} -line for three different deposition conditions: no RF bias with H_2 injected through the nozzle, with RF bias and with H_2 injected through the nozzle, and with RF bias and with H_2 injected through the injection ring.

The change in dilution is achieved by increasing the hydrogen flow through the nozzle. This change in dilution (increasing from samples a1 to a4 and from b1 to b4 in Fig. 1) results in higher crystalline fractions and deposition pressure. The crystalline fraction, microstructure factor, and the deposition pressure are given in Fig. 1.

For RF biased a-Si:H the microstructure factor is higher for unbiased material ($R^* \sim 0.55$ for sample a1) than for biased ($R^* \sim 0.24$ for sample b1) material. We conclude that the material deposited with no RF bias has a higher degree of porosity than material deposited with RF bias. Further, the narrow infrared absorption peak at $2105\text{-}2112\text{ cm}^{-1}$ observed for unbiased amorphous material (see a1 and a2 in Fig. 1(a)) is not observed for biased material. Following Ref. 9, we assign this mode to high hydride configurations on void surfaces. Therefore, we conclude that the density of these configurations is large in unbiased material.

The effect of biasing is also observable for nanocrystalline material, with a similar trend as for a-Si:H: R^* of biased material is significantly lower than for unbiased material, indicating a more compact structure when external RF biasing is used. Further, the integrated absorption of the peak doublet at 2080 and 2100 cm^{-1} is reduced (from 4 cm^{-1} to 2 cm^{-1} , for samples a4 and b4, respectively), possibly an indication of better inter-grain and inter-phase boundaries between the amorphous and the crystals.

The intensity of the H_{α} -line measured for samples (a4) and (b4) is shown in Fig. 2. The presence of an external RF bias for nanocrystalline deposition conditions creates a secondary plasma that might be responsible for the creation of the extra atomic hydrogen measured by OES. The SiH*-line and the intensity ratio of the H_{β} -line over the H_{α} -line, related to the electron temperature, remain unaltered. Additional H ion implantation together with the ion bombardment resulting for the RF biasing may be responsible for densification under RF biasing, as has been previously reported [12].

B. Injection position of H_2 feed gas

With the use of biasing the structure of the material has become more compact, although the microstructure factor is still relatively high ($R^* \sim 0.4$ for sample b4 in Fig. 1). Due to the large distance between the injection of H_2 gas in the nozzle and the substrate holder (45 cm) significant loss of atomic H can occur due to recombination reactions. Assuming that densification of nc-Si:H is a consequence of a higher atomic H density close to the growing surface, we have repeated the series of samples (b) from Fig. 1, modifying the position where the H_2 gas is injected. In the new series (sample (c) in Fig. 1) the H_2 is injected closer to the substrate holder. We expect to reduce loss of atomic hydrogen.

The infra-red spectra of samples with similar crystalline fraction but with different position of H_2 gas injected are shown in Fig. 1 by samples (b4) and (c3). From this figure the mode at 2000 cm^{-1} , assigned to the stretching mode of monohydride (SiH) bonding configuration in the bulk of the material, is significantly increased when H_2 is injected near the substrate. As a result R^* is reduced from 0.39 to 0.31, indicating a reduction in the porosity of the material. This porosity reduction is also confirmed by ellipsometry measurements as shown in Fig. 3. Fig. 3 shows the effect of the H_2 injection position on the imaginary part of the pseudo-dielectric function ($\langle \epsilon_2 \rangle$), measured in situ and extracted from SE data. The amplitude of $\langle \epsilon_2 \rangle$ depends on the crystalline fraction, the crystal size, the surface roughness and the porosity of the material. The shape of $\langle \epsilon_2 \rangle$ remains similar for both samples while the magnitude increases when injecting the H_2 closer to the substrate. These two factors (shape and intensity) suggest a decrease in the void fraction for the material deposited with H_2 injected closer to the substrate.

The intensity of the H_{α} -line measured for samples (b4) and (c3) is shown in Fig. 2. Also in this case the SiH*-line and the intensity ratio of the H_{β} -line over the H_{α} -line remain unaltered. The injection of H_2 close to the substrate generates a higher concentration of atomic H. The additional H ion implantation,

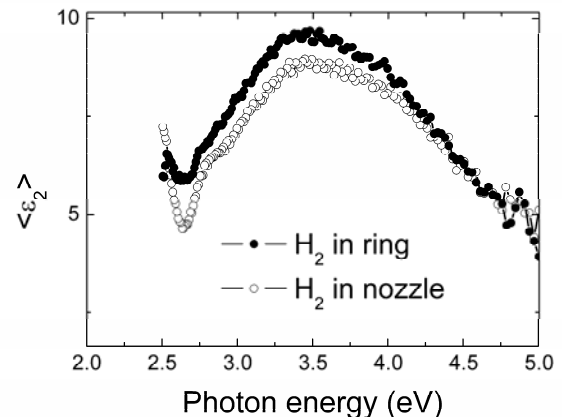


Fig. 3. Effect of the injection position of the H_2 feed gas on the imaginary part of the pseudo-dielectric function of $\langle \epsilon_2 \rangle$ of the nc-Si:H samples with crystalline fraction of $\sim 50\%$.

together with the ion bombardment resulting for the RF biasing may be responsible for the densification under RF biasing [12], as the energy transferred from the ions to the growth surface results in an ordered film structure with lower defect density and film porosity.

In conclusion, a densification of the nc-Si:H deposited by ETP-CVD can be achieved combining external RF bias of the substrate with a higher concentration of atomic hydrogen close to the growth surface. Due to the formation of a secondary plasma when the bias is applied, more insight is needed to clarify the role the RF bias on H₂ dissociation and ion acceleration.

ACKNOWLEDGMENT

The authors would like to acknowledge Martijn Tijssen and Kasper Zwetsloot for the skillful technical assistance. This research was financially supported by SenterNovem.

REFERENCES

- [1] A. Matsuda, *J. Non-Cryst. Solids* 338–340, 1 (2004).
- [2] A. Gordijn, L. Hodakova, J. K. Rath, and R. E. I. Schropp, *J. Non-Cryst. Solids* 352, 1868 (2006).
- [3] M. Kondo, T. Nishimoto, M. Takai, S. Suzuki, Y. Nasuno, and A. Matsuda, *Tech. Dig. Intern. PVSEC-12*, Jeju, Korea, 41 (2001).
- [4] C. Smit, E. A. G. Hamers, B. A. Korevaar, R. A. C. M. M. van Swaaij, and M. C. M. van de Sanden, *J. Non-Cryst. Solids* 299-302, 98 (2002).
- [5] C. Smit, R. A. C. M. M. van Swaaij, E. A. G. Hamers, and M. C. M. van de Sanden, *J. Appl. Phys.* 96, 4076 (2004).
- [6] R. A. C. M. M. van Swaaij, R. Jiménez Zambrano, C. Smit, and M. C. M. van de Sanden, *J. Non-Cryst. Solids* 352, 933 (2006).
- [7] C. Smit, A. Klaver, B. A. Korevaar, A. M. H. N. Petit, D. L. Williamson, R. A. C. M. M. van Swaaij, and M. C. M. van de Sanden, *Thin Solid Films* 491, 280 (2005).
- [8] P. J. Zanzucchi, in: *Semiconductors and Semimetals*, 21, chapter 4 (1984).
- [9] S. Agarwal, A. Takano, M. C. M. van de Sanden, D. Maroudas, and E. S. Aydil, *J. Chem. Phys.* 117, 10805 (2002).
- [10] A. H. M. Smets, W. M. M. Kessels, and M. C. M. van de Sanden, *Appl. Phys. Lett.* 86, 041909 (2005).
- [11] R. Jimenez Zambrano, R. A. C. M. M. van Swaaij, and M. C. M. van de Sanden, *Mater. Res. Soc. Symp. Proc.* 989, accepted for publication (2007).
- [12] B. Kalache, A. I. Kosarev, R. Vanderhaghen, and P. Roca i Cabarrocas, *J. Appl. Phys.* 93, 1262 (2002).